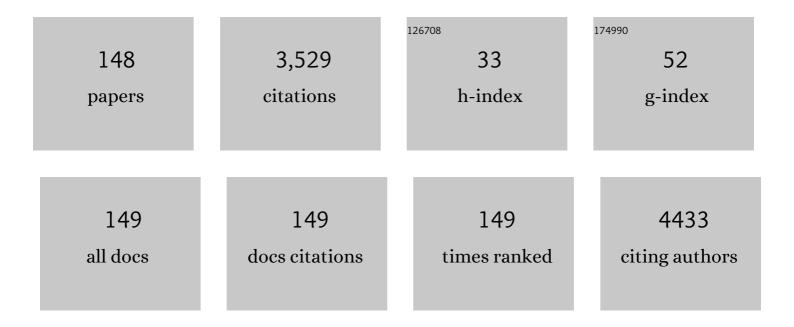
List of Publications by Year in descending order

Source: https://exaly.com/author-pdf/7970257/publications.pdf Version: 2024-02-01



#	Article	IF	CITATIONS
1	Prognostic Value of Interim 18F-DOPA and 18F-FDG PET/CT Findings in Stage 3–4 Pediatric Neuroblastoma. Clinical Nuclear Medicine, 2022, 47, 21-25.	0.7	4
2	Neuroinflammation in Low-Level PM2.5-Exposed Rats Illustrated by PET via an Improved Automated Produced [ <sup>18</sup> F]FEPPA: A Feasibility Study. Molecular Imaging, 2022, 2022, .	0.7	1
3	Effects of Focal Radiation on [18F]-Fluoro-D-Glucose Positron Emission Tomography in the Brains of Miniature Pigs: Preliminary Findings on Local Metabolism. Neuromodulation, 2021, 24, 863-869.	0.4	7
4	Endoscopic ultrasound ablation in a patient with multiple metastatic pancreatic tumors from adrenocorticotropic hormoneâ€producing thymic neuroendocrine neoplasm. Digestive Endoscopy, 2021, 33, 458-463.	1.3	2
5	A <scp>Doubleâ€Blind</scp> , Randomized, Controlled Trial of Lovastatin in <scp>Earlyâ€Stage</scp> Parkinson's Disease. Movement Disorders, 2021, 36, 1229-1237.	2.2	22
6	Integrated 18F-T807 Tau PET, Structural MRI, and Plasma Tau in Tauopathy Neurodegenerative Disorders. Frontiers in Aging Neuroscience, 2021, 13, 646440.	1.7	13
7	NP-59 Adrenal Scintigraphy as an Imaging Biomarker to Predict KCNJ5 Mutation in Primary Aldosteronism Patients. Frontiers in Endocrinology, 2021, 12, 644927.	1.5	4
8	Preoperative 2-[18F]FDG PET-CT aids in the prognostic stratification for patients with primary ampullary carcinoma. European Radiology, 2021, 31, 8040-8049.	2.3	4
9	Assessing tumor angiogenesis using dynamic contrast-enhanced integrated magnetic resonance-positron emission tomography in patients with non-small-cell lung cancer. BMC Cancer, 2021, 21, 348.	1.1	6
10	Centrum Semiovale Perivascular Space and Amyloid Deposition in Spontaneous Intracerebral Hemorrhage. Stroke, 2021, 52, 2356-2362.	1.0	23
11	Diagnostic Performance of Proton Magnetic Resonance Spectroscopy and 18F-Fluorocholine PET to Differentiate Benign From Malignant Breast Lesions. Clinical Nuclear Medicine, 2021, Publish Ahead of Print, 896-903.	0.7	3
12	Plasma soluble TREM2 is associated with white matter lesions independent of amyloid and tau. Brain, 2021, 144, 3371-3380.	3.7	19
13	Taiwan mini-frontier of primary aldosteronism: Updating treatment and comorbidities detection. Journal of the Formosan Medical Association, 2021, 120, 1811-1820.	0.8	5
14	Diagnostic Effect of Attenuation Correction in Myocardial Perfusion Imaging in Different Coronary Arteries: A Systematic Review and Meta-Analysis. Frontiers in Cardiovascular Medicine, 2021, 8, 756060.	1.1	1
15	Factors predicting one or two sentinel lymph nodes to be accepted for sentinel lymph node biopsy alone after neoadjuvant therapy in initially node-positive breast cancer patients. Surgical Oncology, 2021, 39, 101667.	0.8	0
16	Long-term prognostic value of computed tomography-based attenuation correction on thallium-201 myocardial perfusion imaging: A cohort study. PLoS ONE, 2021, 16, e0258983.	1.1	5
17	2021 Advocacy Statements for the Role of Tc-Pyrophosphate Scintigraphy in the Diagnosis of Transthyretin Cardiac Amyloidosis: A Report of the Taiwan Society of Cardiology and the Society of Nuclear Medicine of the Republic of China. Acta Cardiologica Sinica, 2021, 37, 221-231.	0.1	2
18	Clinical significance of quantitative assessment of glucose utilization in patients with ischemic cardiomyopathy. Journal of Nuclear Cardiology, 2020, 27, 269-279.	1.4	9

#	Article	IF	CITATIONS
19	Three-step two-pot automated production of NCA [18F]FDOPA with FlexLab module. Applied Radiation and Isotopes, 2020, 158, 108871.	0.7	5
20	Superficial Cerebellar Microbleeds and Cerebral Amyloid Angiopathy. Stroke, 2020, 51, 202-208.	1.0	40
21	Mitochondrial <i>UQCRC1</i> mutations cause autosomal dominant parkinsonism with polyneuropathy. Brain, 2020, 143, 3352-3373.	3.7	37
22	Transtubular potassium gradient predicts kidney function impairment after adrenalectomy in primary aldosteronism. Therapeutic Advances in Chronic Disease, 2020, 11, 204062232094479.	1.1	1
23	Dermoid cyst with secretion of CA 19-9 detected by 18F-FDG PET/CT. Medicine (United States), 2020, 99, e18988.	0.4	3
24	Frontal variant of Alzheimer's disease with asymmetric presentation mimicking frontotemporal dementia: Case report and literature review. Brain and Behavior, 2020, 10, e01548.	1.0	18
25	An one-pot two-step automated synthesis of [18F]T807 injection, its biodistribution in mice and monkeys, and a preliminary study in humans. PLoS ONE, 2019, 14, e0217384.	1.1	3
26	Microangiopathy underlying mixed-location intracerebral hemorrhages/microbleeds. Neurology, 2019, 92, e774-e781.	1.5	63
27	Plasma Aldosterone After Seated Saline Infusion Test Outperforms Captopril Test at Predicting Clinical Outcomes After Adrenalectomy for Primary Aldosteronism. American Journal of Hypertension, 2019, 32, 1066-1074.	1.0	12
28	Advances in cerebral amyloid angiopathy imaging. Therapeutic Advances in Neurological Disorders, 2019, 12, 175628641984411.	1.5	24
29	Predicting tumor responses and patient survival in chemoradiotherapy-treated patients with non-small-cell lung cancer using dynamic contrast-enhanced integrated magnetic resonance–positron-emission tomography. Strahlentherapie Und Onkologie, 2019, 195, 707-718.	1.0	10
30	Improved diagnostic accuracy of thallium-201 myocardial perfusion single-photon emission computed tomography with CT attenuation correction. Journal of Nuclear Cardiology, 2019, 26, 1584-1595.	1.4	13
31	Targeted treatment of primary aldosteronism – The consensus of Taiwan Society of Aldosteronism. Journal of the Formosan Medical Association, 2019, 118, 72-82.	0.8	25
32	Multiparametric PET/MR imaging biomarkers are associated with overall survival in patients with pancreatic cancer. European Journal of Nuclear Medicine and Molecular Imaging, 2018, 45, 1205-1217.	3.3	35
33	Clinical Utility of FDG PET/CT in Patients with Autoimmune Pancreatitis: a Case-Control Study. Scientific Reports, 2018, 8, 3651.	1.6	38
34	Distribution of Lacunar Infarcts in Asians With Intracerebral Hemorrhage. Stroke, 2018, 49, 1515-1517.	1.0	22
35	Response assessment of stereotactic body radiation therapy using dynamic contrastâ€enhanced integrated MRâ€PET in nonâ€small cell lung cancer patients. Journal of Magnetic Resonance Imaging, 2018, 47, 191-199.	1.9	19
36	Targeting histone deacetylase 4/ubiquitinâ€conjugating enzyme 9 impairs DNA repair for radiosensitization of hepatocellular carcinoma cells in mice. Hepatology, 2018, 67, 586-599.	3.6	29

#	Article	IF	CITATIONS
37	Impact of initial myocardial perfusion imaging versus invasive coronary angiography on outcomes in coronary artery disease: a nationwide cohort study. European Journal of Nuclear Medicine and Molecular Imaging, 2018, 45, 567-574.	3.3	9
38	The Relation Between Brain Amyloid Deposition, Cortical Atrophy, and Plasma Biomarkers in Amnesic Mild Cognitive Impairment and Alzheimer's Disease. Frontiers in Aging Neuroscience, 2018, 10, 175.	1.7	48
39	Surgical outcomes of patients with primary aldosteronism lateralized with I-131-6 β-iodomethyl-norcholesterol single photon emission/computed tomography without discontinuation or modification of antihypertensive medications. Tzu Chi Medical Journal, 2018, 30, 169.	0.4	0
40	Multiparametric Evaluation of Treatment Response to Neoadjuvant Chemotherapy in Breast Cancer Using Integrated PET/MR. Clinical Nuclear Medicine, 2017, 42, 506-513.	0.7	28
41	Ictal Phase Perfusion SPECT of Nonketotic Hyperglycemia-Induced Parieto-occipital Seizure. Clinical Nuclear Medicine, 2017, 42, e67-e68.	0.7	4
42	Diagnostic and Prognostic Implications of Exercise Treadmill and Rest First-Pass Radionuclide Angiography in Patients With Pulmonary Hypertension. Clinical Nuclear Medicine, 2017, 42, e392-e399.	0.7	3
43	Correlation of Cerebral Microbleed Distribution to Amyloid Burden in Patients with Primary Intracerebral Hemorrhage. Scientific Reports, 2017, 7, 44715.	1.6	37
44	Case detection and diagnosis of primary aldosteronism – The consensus of Taiwan Society of Aldosteronism. Journal of the Formosan Medical Association, 2017, 116, 993-1005.	0.8	85
45	Risk Stratification of Pediatric Patients With Neuroblastoma Using Volumetric Parameters of 18F-FDG and 18F-DOPA PET/CT. Clinical Nuclear Medicine, 2017, 42, e142-e148.	0.7	32
46	Increased risk of dementia in patients hospitalized with acute kidney injury: A nationwide population-based cohort study. PLoS ONE, 2017, 12, e0171671.	1.1	28
47	Increased heterogeneity of brain perfusion is an early marker of central nervous system involvement in antiphospholipid antibody carriers. PLoS ONE, 2017, 12, e0182344.	1.1	2
48	The relationship between serum fibrosis markers and restrictive ventricular filling in patients with heart failure with reduced ejection fraction: A technetium-99m radionuclide ventriculography study. Oncotarget, 2017, 8, 2381-2390.	0.8	4
49	A multidisciplinary team care approach improves outcomes in high-risk pediatric neuroblastoma patients. Oncotarget, 2017, 8, 4360-4372.	0.8	19
50	Longitudinal evaluation of myocardial glucose metabolism and contractile function in obese type 2 diabetic db/db mice using small-animal dynamic 18F-FDG PET and echocardiography. Oncotarget, 2017, 8, 87795-87808.	0.8	11
51	Clinical significance of right ventricular activity on treadmill thallium-201 myocardial single-photon emission computerized tomography using cadmium–zinc–telluride cameras. Nuclear Medicine Communications, 2016, 37, 650-657.	0.5	8
52	Pregnancy Incidence in Female Nasopharyngeal Carcinoma Survivors of Reproductive Age. Medicine (United States), 2016, 95, e3729.	0.4	3
53	Pregnancy Outcome After I-131 Therapy for Patients With Thyroid Cancer. Medicine (United States), 2016, 95, e2685.	0.4	19
54	Diagnostic Performance of Attenuation-Corrected Myocardial Perfusion Imaging for Coronary Artery Disease: A Systematic Review and Meta-Analysis. Journal of Nuclear Medicine, 2016, 57, 1893-1898.	2.8	51

#	Article	IF	CITATIONS
55	18F-NaF PET/CT Images of Cardiac Metastasis From Osteosarcoma. Clinical Nuclear Medicine, 2016, 41, 708-709.	0.7	17
56	Intratumoral Heterogeneity of Pretreatment 18F-FDG PET Images Predict Disease Progression in Patients With Nasal Type Extranodal Natural Killer/T-cell Lymphoma. Clinical Nuclear Medicine, 2016, 41, 922-926.	0.7	29
57	Hepatitis C virus infection as a risk factor for Parkinson disease. Neurology, 2016, 86, 840-846.	1.5	63
58	A Novel Potential Positron Emission Tomography Imaging Agent for Vesicular Monoamine Transporter Type 2. PLoS ONE, 2016, 11, e0161295.	1.1	6
59	New Trends in Radionuclide Myocardial Perfusion Imaging. Acta Cardiologica Sinica, 2016, 32, 156-66.	0.1	11
60	Follicular thyroid carcinoma with NRAS Q61K and GNAS R201H mutations that had a good 131I treatment response. Endocrinology, Diabetes and Metabolism Case Reports, 2016, 2016, 150067.	0.2	3
61	The Incremental Diagnostic Performance of Coronary Computed Tomography Angiography Added to Myocardial Perfusion Imaging in Patients with Intermediate-to-High Cardiovascular Risk. Acta Cardiologica Sinica, 2016, 32, 145-55.	0.1	11
62	SVM based lung cancer diagnosis using multiple image features in PET/CT. , 2015, , .		4
63	Standardized uptake value and apparent diffusion coefficient of endometrial cancer evaluated with integrated wholeâ€body PET/MR: Correlation with pathological prognostic factors. Journal of Magnetic Resonance Imaging, 2015, 42, 1723-1732.	1.9	45
64	Patterns of Nodal Metastases on 18F-FDG PET/CT in Patients With Esophageal Squamous Cell Carcinoma are Useful to Guide Treatment Planning of Radiotherapy. Clinical Nuclear Medicine, 2015, 40, 384-389.	0.7	7
65	A performance comparison of novel cadmium–zinc–telluride camera and conventional SPECT/CT using anthropomorphic torso phantom and water bags to simulate soft tissue and breast attenuation. Annals of Nuclear Medicine, 2015, 29, 342-350.	1.2	33
66	Data-driven respiratory motion tracking and compensation in CZT cameras: A comprehensive analysis of phantom and human images. Journal of Nuclear Cardiology, 2015, 22, 308-318.	1.4	34
67	131I treatment for thyroid cancer and the risk of developing salivary and lacrimal gland dysfunction and a second primary malignancy: a nationwide population-based cohort study. European Journal of Nuclear Medicine and Molecular Imaging, 2015, 42, 1172-1178.	3.3	36
68	The value of losartan suppression test in the confirmatory diagnosis of primary aldosteronism in patients over 50 years old. JRAAS - Journal of the Renin-Angiotensin-Aldosterone System, 2015, 16, 587-598.	1.0	9
69	Incremental Diagnostic Performance of Combined Parameters in the Detection of Severe Coronary Artery Disease Using Exercise Gated Myocardial Perfusion Imaging. PLoS ONE, 2015, 10, e0134485.	1.1	9
70	Using 18F-FLT PET to distinguish between malignant and benign breast lesions with suspicious findings in mammography and breast ultrasound. Annals of Nuclear Medicine, 2014, 28, 941-949.	1.2	5
71	Most frequent location of the sentinel lymph nodes. Asian Journal of Surgery, 2014, 37, 125-129.	0.2	8
72	Prognostic value of semiquantification NP-59 SPECT/CT in primary aldosteronism patients after adrenalectomy. European Journal of Nuclear Medicine and Molecular Imaging, 2014, 41, 1375-1384.	3.3	22

#	Article	IF	CITATIONS
73	Neuroimaging and electroencephalographic changes after vagus nerve stimulation in a boy with medically intractable myoclonic astatic epilepsy. Journal of the Formosan Medical Association, 2014, 113, 258-263.	0.8	8
74	The utilization of radionuclide myocardial perfusion imaging and cardiac catheterization under Taiwan's universal health insurance program. International Journal of Cardiovascular Imaging, 2013, 29, 1039-1042.	0.7	0
75	Increased risk of acute coronary syndrome after spinal cord injury: A nationwide 10-year follow-up cohort study. International Journal of Cardiology, 2013, 168, 1681-1682.	0.8	9
76	Mystery Case: Hemiballism in a patient with parietal lobe infarction. Neurology, 2013, 80, e22.	1.5	4
77	67Ga SPECT/CT Aids in the Diagnosis of Occult Infected Common Iliac Artery Aneurysm. Clinical Nuclear Medicine, 2013, 38, 573-575.	0.7	4
78	High 18F-Fluorothymidine Uptake for Invasive Thymoma. Clinical Nuclear Medicine, 2012, 37, 991-992.	0.7	1
79	High false negative rate of Tc-99m MDP whole-body bone scintigraphy in detecting skeletal metastases for patients with hepatoma. Journal of the Formosan Medical Association, 2012, 111, 140-146.	0.8	15
80	The effects of 3-month atorvastatin therapy on arterial inflammation, calcification, abdominal adipose tissue and circulating biomarkers. European Journal of Nuclear Medicine and Molecular Imaging, 2012, 39, 399-407.	3.3	92
81	The Association of Infrared Imaging Findings of the Breast with Hormone Receptor and Human Epidermal Growth Factor Receptor 2 Status of Breast Cancer. Academic Radiology, 2011, 18, 212-219.	1.3	7
82	Kidney impairment in primary aldosteronism. Clinica Chimica Acta, 2011, 412, 1319-1325.	0.5	112
83	Neuroimaging Findings in a Brain With Niemann–Pick Type C Disease. Journal of the Formosan Medical Association, 2011, 110, 537-542.	0.8	36
84	Diagnostic value of 18F-FDC-PET/CT in indeterminate infiltrative hepatic lesions in an endemic area of viral hepatitis. Nuclear Medicine Communications, 2011, 32, 252-259.	0.5	3
85	F-18 FDG PET Images for Subcutaneous Panniculitis-like T-Cell Lymphoma. Clinical Nuclear Medicine, 2011, 36, 66-69.	0.7	59
86	Gallium-67 SPECT/CT for Abdominal Abscess. Clinical Nuclear Medicine, 2011, 36, 258-260.	0.7	6
87	The association of serum potassium level with left ventricular mass in patients with primary aldosteronism. European Journal of Clinical Investigation, 2011, 41, 743-750.	1.7	33
88	Factors influencing left ventricular mass regression in patients with primary aldosteronism post adrenalectomy. JRAAS - Journal of the Renin-Angiotensin-Aldosterone System, 2011, 12, 48-53.	1.0	30
89	Unusual presentation of multiple pathologic bone fractures in a patient with gastric mucosa-associated lymphoid tissue lymphoma. Annals of Hematology, 2010, 89, 431-436.	0.8	1
90	The diagnostic and prognostic effectiveness of F-18 sodium fluoride PET-CT in detecting bone metastases for hepatocellular carcinoma patients. Nuclear Medicine Communications, 2010, 31, 637-645.	0.5	55

#	Article	IF	CITATIONS
91	PET Assessment of Myocardial Perfusion Reserve Inversely Correlates with Intravascular Ultrasound Findings in Angiographically Normal Cardiac Transplant Recipients. Journal of Nuclear Medicine, 2010, 51, 906-912.	2.8	67
92	Diagnosis of primary aldosteronism: Comparison of post-captopril active renin concentration and plasma renin activity. Clinica Chimica Acta, 2010, 411, 657-663.	0.5	36
93	<sup>131</sup> I-6β-Iodomethyl-19-Norcholesterol SPECT/CT for Primary Aldosteronism Patients with Inconclusive Adrenal Venous Sampling and CT Results. Journal of Nuclear Medicine, 2009, 50, 1631-1637.	2.8	103
94	Association of Kidney Function With Residual Hypertension After Treatment of Aldosterone-Producing Adenoma. American Journal of Kidney Diseases, 2009, 54, 665-673.	2.1	93
95	Usefulness of <sup>201</sup> TL SPECT/CT relative to <sup>18</sup> Fâ€FDG PET/CT in detecting recurrent skull base nasopharyngeal carcinoma. Head and Neck, 2009, 31, 717-724.	0.9	8
96	Asymptomatic Thymic Carcinoma With Solitary Hepatic Metastasis Detected by Fluorodeoxyglucose Positron Emission Tomography. Journal of the Formosan Medical Association, 2009, 108, 677-680.	0.8	2
97	The Cost-utility Analysis of 18-Fluoro-2-Deoxyglucose Positron Emission Tomography in the Diagnosis of Recurrent Nasopharyngeal Carcinoma. Academic Radiology, 2009, 16, 54-60.	1.3	29
98	Abnormal Myocardial Perfusion Imaging After Percutaneous Coronary Intervention Without Obstructing Lesion. Clinical Nuclear Medicine, 2009, 34, 38-39.	0.7	0
99	18F-FDG PET for the lymph node staging of non-small cell lung cancer in a tuberculosis-endemic country: Is dual time point imaging worth the effort?. European Journal of Nuclear Medicine and Molecular Imaging, 2008, 35, 1305-1315.	3.3	68
100	Interactive 3D Hybrid PET/CT Imaging in the Identification of Myocardial Viability in Patients After Myocardial Infarction: Feasibility Study and Clinical Implications. Journal of the Formosan Medical Association, 2008, 107, 470-477.	0.8	1
101	Intravascular Ultrasound Correlates with Coronary Flow Reserve and Predicts the Survival in Angiographically Normal Cardiac Transplant Recipients. Cardiology, 2008, 109, 93-98.	0.6	18
102	Usefulness of Lymphoscintigraphy in Demonstrating Lymphedema in Patients With Noonan Syndrome. Clinical Nuclear Medicine, 2008, 33, 226-227.	0.7	4
103	Myocardial Perfusion Imaging of Subacute Stent Thrombosis After Percutaneous Coronary Intervention. Clinical Nuclear Medicine, 2008, 33, 414-415.	0.7	1
104	F-18 Fluorodeoxyglucose Uptake in Gastric Adenoma After Stomach Distention by Water. Clinical Nuclear Medicine, 2008, 33, 643-644.	0.7	0
105	F-18 FDG PET/CT Illustrating Tumor Invasion in the IVC From Adrenocortical Carcinoma. Clinical Nuclear Medicine, 2007, 32, 891-892.	0.7	5
106	Bilateral subthalamotomy for advanced Parkinson disease. World Neurosurgery, 2007, 68, S43-S50.	1.3	30
107	Extensive scar myocardium in hypertrophic cardiomyopathy with severe myocardial bridge. International Journal of Cardiology, 2007, 115, e105-e107.	0.8	7
108	Radio-guided Sentinel Lymph Node Biopsy Using Periareolar Injection Technique for Patients with Early Breast Cancer. Journal of the Formosan Medical Association, 2007, 106, 44-50.	0.8	8

#	Article	IF	CITATIONS
109	Characterization of plaques using 18F-FDG PET/CT in patients with carotid atherosclerosis and correlation with matrix metalloproteinase-1. Journal of Nuclear Medicine, 2007, 48, 227-33.	2.8	66
110	Network modulation by the subthalamic nucleus in the treatment of Parkinson's disease. NeuroImage, 2006, 31, 301-307.	2.1	151
111	The relation of amino-terminal propeptide of type III procollagen and severity of coronary artery disease in patients without myocardial infarction or hibernation. Clinical Biochemistry, 2006, 39, 861-866.	0.8	23
112	Assessment of myocardial viability using F-18 fluorodeoxyglucose/Tc-99m sestamibi dual-isotope simultaneous acquisition SPECT: Comparison with Tl-201 stress-reinjection SPECT. Journal of Nuclear Cardiology, 2005, 12, 451-459.	1.4	15
113	Early restaging whole-body 18F-FDG PET during induction chemotherapy predicts clinical outcome in patients with locoregionally advanced nasopharyngeal carcinoma. European Journal of Nuclear Medicine and Molecular Imaging, 2005, 32, 1152-1159.	3.3	46
114	Usefulness of Progressive Inhomogeneity of Myocardial Perfusion and Chronotropic Incompetence in Detecting Cardiac Allograft Vasculopathy: Evaluation with Dobutamine Thallium-201 Myocardial SPECT. Cardiology, 2005, 104, 156-161.	0.6	7
115	Diagnostic and Prognostic Value of Dobutamine Thallium-201 Single-Photon Emission Computed Tomography After Heart Transplantation. Journal of Heart and Lung Transplantation, 2005, 24, 544-550.	0.3	53
116	Whole-body 18F-FDG PET in recurrent or metastatic nasopharyngeal carcinoma. Journal of Nuclear Medicine, 2005, 46, 770-4.	2.8	42
117	Lack of independent relationship between plasma adiponectin, leptin levels and bone density in nondiabetic female adolescents. Clinical Endocrinology, 2004, 61, 204-208.	1.2	62
118	Plasma Adiponectin Levels and Metabolic Factors in Nondiabetic Adolescents. Obesity, 2004, 12, 119-124.	4.0	59
119	The relation between myocardial cyclic variation of integrated backscatter and serum concentrations of procollagen propeptides in hypertensive patients. Ultrasound in Medicine and Biology, 2004, 30, 885-891.	0.7	31
120	Using 18-fluoro-2-deoxyglucose positron emission tomography in detecting infectious endocarditis/endoarteritis. Academic Radiology, 2004, 11, 316-321.	1.3	54
121	FDG PET Manifestation of Lobular Panniculitis. Clinical Nuclear Medicine, 2004, 29, 442-443.	0.7	5
122	Gallium-67 Scintigraphy and F-18 Fluorodeoxyglucose Position Emission Tomography in Posttransplant Lymphoproliferative Disorder. Clinical Nuclear Medicine, 2004, 29, 329-331.	0.7	4
123	Comparison of gallium-67 citrate and technetium-99m tetrofosmin scan to detect Hodgkin's disease. Annals of Nuclear Medicine, 2003, 17, 439-442.	1.2	1
124	High prevalence of asymptomatically poor muscle perfusion of lower extremities measured in type II diabetes patients with abnormal myocardial perfusion. Journal of Diabetes and Its Complications, 2003, 17, 365-368.	1.2	3
125	18-Fluoro-2-deoxyglucose positron emission tomography in detecting residual/recurrent nasopharyngeal carcinomas and comparison with magnetic resonance imaging. Cancer, 2003, 98, 283-287.	2.0	98
126	Using thallium-201 SPECT to detect recurrent or residual nasopharyngeal carcinoma after radiotherapy in patients with indeterminate CT findings. Head and Neck, 2003, 25, 645-648.	0.9	6

#	Article	IF	CITATIONS
127	Treatment of advanced Parkinson's disease by subthalamotomy: One-year results. Movement Disorders, 2003, 18, 531-538.	2.2	66
128	Tl-201 myocardial SPECT in differentiation of ischemic from nonischemic dilated cardiomyopathy in patients with left ventricular dysfunction. Journal of Nuclear Cardiology, 2003, 10, 369-374.	1.4	35
129	Compare FDG-PET and Tc-99m tetrofosmin SPECT to detect metastatic thyroid carcinoma1. Academic Radiology, 2003, 10, 835-839.	1.3	20
130	Usefulness of Tc-99m HMPAO-labeled WBC heart scan to predict impaired ventricular function and coronary artery dilation in children with Kawasaki disease. International Journal of Cardiology, 2003, 92, 65-69.	0.8	3
131	Differentiating Solitary Pulmonary Metastases in Patients with Extrapulmonary Neoplasmas Using FDG–PET. Cancer Investigation, 2003, 21, 47-52.	0.6	11
132	Tcâ€99m MIBI SPECT in Detecting Metastatic Papillary Thyroid Carcinoma in Patients with Elevated Human Serum Thyroglobulin Levels but Negative Iâ€131 Whole Body Scan. Endocrine Research, 2003, 29, 9-15.	0.6	11
133	Evolving metabolic changes during the first postoperative year after subthalamotomy. Journal of Neurosurgery, 2003, 99, 872-878.	0.9	31
134	Aortic Dissection Detected on Three-Phase Bone Scintigraphy. Clinical Nuclear Medicine, 2003, 28, 858-860.	0.7	1
135	Fluorine-18 FDG-PET in Detecting Local Recurrence and Distant Metastases in Breast Cancer—Taiwanese Experiences. Cancer Investigation, 2002, 20, 725-729.	0.6	21
136	Subthalamotomy for advanced Parkinson disease. Journal of Neurosurgery, 2002, 97, 598-606.	0.9	48
137	Predicting Chemotherapy Response to Paclitaxel-Based Therapy in Advanced Non-Small-Cell Lung Cancer (Stage IIIb or IV) with a Higher T Stage (> T2). Oncology, 2002, 63, 173-179.	0.9	12
138	Clinical Impact of [18F]FDG-PET in Patients with Suspected Recurrent Breast Cancer Based on Asymptomatically Elevated Tumor Marker Serum Levels: a Preliminary Report. Japanese Journal of Clinical Oncology, 2002, 32, 244-247.	0.6	48
139	Detection of recurrent or persistent nasopharyngeal carcinomas after radiotherapy with technetium-99m methoxyisobutylisonitrile single photon emission computed tomography and computed tomography. Cancer, 2002, 94, 1981-1986.	2.0	49
140	False-positive uptake of 18F-fluorodeoxyglucose in the hilar region and mediastinum. Seminars in Nuclear Medicine, 2001, 31, 84-86.	2.5	4
141	Assessment of the myocardial changes in heart transplant recipients without evident acute myocardial rejection by integrated backscatter: comparison with simultaneous dobutamine stress echocardiography and 201thallium spect. Ultrasound in Medicine and Biology, 2001, 27, 171-179.	0.7	6
142	Accuracy of biphasic response, sustained improvement and worsening during dobutamine echocardiography in predicting recovery of resting myocardial dysfunction after revascularization: comparison with thallium-201 SPECT. Ultrasound in Medicine and Biology, 2001, 27, 925-931.	0.7	5
143	Comparing 18-fluoro-2-deoxyglucose positron emission tomography with a combination of technetium 99m tetrofosmin single photon emission computed tomography and computed tomography to detect recurrent or persistent nasopharyngeal carcinomas after radiotherapy. Cancer, 2001, 92, 434-439.	2.0	30
144	Metabolic changes following subthalamotomy for advanced Parkinson's disease. Annals of Neurology, 2001, 50, 514-520.	2.8	89

#	Article	IF	CITATIONS
145	Ultrasonic tissue characterization evaluates myocardial viability and ischemia in patients with coronary artery disease. Ultrasound in Medicine and Biology, 2000, 26, 759-769.	0.7	11
146	Comparison of 18-Fluoro-2-Deoxyglucose Positron Emission Tomography and Computed Tomography in Detection of Cervical Lymph Node Metastases of Nasopharyngeal Carcinoma. Annals of Otology, Rhinology and Laryngology, 2000, 109, 1130-1134.	0.6	36
147	Significance of dobutamine-induced ST-segment elevation and T-wave pseudonormalization in patients with Q-wave myocardial infarction: simultaneous evaluation by dobutamine stress echocardiography and thallium-201 SPECT. American Journal of Cardiology, 1999, 84, 125-129.	0.7	21
148	Do β-blockers affect the diagnostic sensitivity of dobutamine stress thallium-201 single photon emission computed tomographic imaging?. Journal of Nuclear Cardiology, 1998, 5, 34-39.	1.4	20